JP1.18 DETECTING MULTILAYER CLOUDS USING SATELLITE SOLAR AND IR CHANNELS

Kazuaki Kawamoto
Research Institute for Humanity and Nature, Kyoto, 606-8502, Japan

Patrick Minnis, William L. Smith, Jr.
NASA Langley Research Center, Hampton, VA 23681

Anita Rapp
AS&M, Hampton, VA 23666

1. INTRODUCTION

Accurate knowledge of the vertical and horizontal distributions of clouds is critical for improving and verifying weather and climate models that either specify or generate realistic cloud fields. Satellite remote sensing has been used for many years to derive cloud properties (e.g. Han *et al*. 1994, Minnis *et al*. 1998). Methods for converting satellite solar and infrared imager data into parameters such as cloud amount, height, optical depth, and particle size traditionally assume that the viewed scene contains a plane-parallel, single-layered cloud. Because multilayered cloud systems are quite common (e.g. Tian and Curry 1989), these basic assumptions are often violated prompting development of methods to detect multilayered clouds (e.g., Baum and Spinhirne 2000, Lin et al. 1999). Many satellite observations of clouds are affected by radiation from more than one cloud layer. As such, cloud overlap can cause errors in the retrieval of many properties including cloud height, optical depth, phase, and particle size. Application of retrieval algorithms that account for more than one layer in a pixel first requires identification of those radiances affected by multilayered clouds.

To shed further light on the characteristics of multilayered clouds, this paper explores the potential for using a combination of direct and indirect measurements from solar and infrared radiances to detect pixels with multilayered clouds. The satellite imager 11 and 12-µm brightness temperature difference BTD has long been used to identify thin cirrus clouds (e.g., Inoue 1985). Typically, the BTD is greater for optically thin cirrus clouds than for either thick clouds or clear skies. Thin cirrus over low-level clouds should also produce a similar signal. Multilayered clouds often yield retrieved cloud properties that represent some value between those for the two separate layers. For example, Han et al. (1994) demonstrated that contamination of the 3.7-µm radiance due to the presence of ice crystals tends to raise the value of effective water droplet radius r_e derived from 3.7-µm data because water droplets have a greater albedo than ice crystals of the same size. Similarly, if the cloud phase is identified as ice, the derived ice crystal effective diameter D_e will be smaller in overlapped conditions than for a single-layered cirrus. Such effects may provide a basis for detecting multilayered clouds. This paper examines the relationships between τ and simultaneous values of BTD, r_e, and D_e to determine empirically if these quantities differ significantly for overlapped and single-layered cloud systems.

*Corresponding author address: Kazuaki Kawamoto, Research Institute for Humanity and Nature, Kyoto, 606-8502, Japan. email: kawamoto@chikyu.ac.jp.

2. DATA

Cloud properties, including τ, effective cloud temperature T_c and r_e or D_e, cloud phase, and other quantities, were derived by Minnis *et al.* (2001) over the Atmospheric Radiation Measurement (ARM) Southern Great Plains Central Facility (SCF) from half-hourly daytime Geostationary Operational Environmental Satellite (GOES-8) 4-km data. The parameters were derived using radiances from the visible (VIS; 0.65 µm), solar-infrared (SI; 3.9 µm), infrared (IR; 10.8 µm), and split-window (SWC; 12.0 µm) channels in the VIS-IR-SI-SWC technique or VISST, an updated version of the 3-channel daytime method described by Minnis *et al.* (1995). It uses the emittance parameterizations of Minnis *et al.* (1998) and VIS reflectance model of Arduini et al. (2002). The cloud properties were derived for all available data between 1 January and 31 December 1998 when the solar zenith angle was less than 78°. The pixel-level results were averaged over a 0.3° box centered on the SCF. Minnis *et al.* (2001) and Dong *et al.* (2002) discuss the validation of the derived cloud properties. The mean BTD value was computed for all cloudy pixels in the 0.3° box for each case.

Fig. 1. Example of radar imagery at SCF (from website of G. Mace at University of Utah)

Cloud boundaries were determined over the SCF at

a vertical resolution of 90 m from a combination of lidar, radar, and ceilometer data by Clothiaux *et al.* (1999). These boundaries were used to determine the presence of single and multilayered clouds during each 10-minute period centered on a given GOES-8 image time. Figure 1 shows a time-series of radar reflectivity over the SCF and the boundaries of the clouds. The 3643 10-minute segments of cloud boundary data that matched the GOES retrievals were classified into four basic exclusive

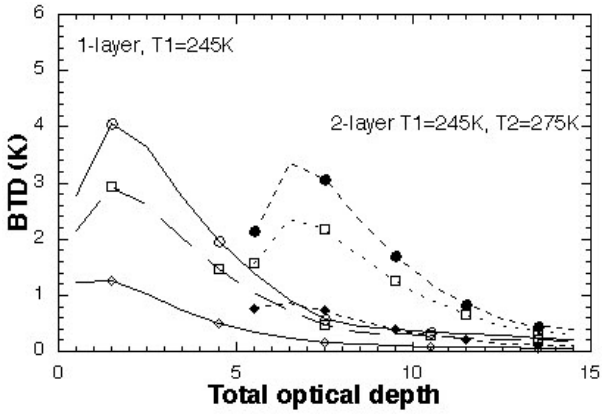

Fig. 2. Theoretical variation of BTD for 1 and 2-layered clouds. Ice cloud: D_e = 24 (circle), 45 (square), 123 µm (diamond).

categories: clear (4.2%), precipitating (27.2%), single-layered (18.5%), and multi-layered (12.9%). Clouds were assumed to be precipitating if radar reflectivities in the lowest layer exceeded -20 dBZ. Such returns are usually indicative of ice or precipitation-sized particles in many cases. The single-layered clouds were divided into two groups: those with tops above and below 4 km. Of the 472 multi-layered systems, 147 were two-layered cloud systems with the upper-layer top above 6 km and the lower-layer top below 4 km. Three or more layers occurred simultaneously in 308 (8.5%) of the cases.

To simplify the analysis, only two-layer cloud systems comprising a thick boundary-layer water cloud lower than 4km overlaid by optically thin ice cloud higher than 6 km are used here. To minimize the occurrence of thick cirrus over lower clouds, it was assumed that the GOES cloud-height retrieval was within 1 km of the radar-derived cloud top altitude for optically thick clouds. Thus, the only GOES retrievals used for two-layer classifications have satellite-derived cloud heights that are lower than the radar-derived upper-cloud top by 1 km or more.

.3. RESULTS

Figure 2 shows an example of *BTD* simulated with the parameterization of Minnis et al. (1998) for a cirrus cloud at a temperature of T1 = 245 K with variable D_e over a surface with a temperature of 290 K. The *BTD* is also simulated for the same cloud over a low-level water cloud at T2 = 275 K with an r_e = 10 µm. Several trends are evident in this figure. BTD decreases with increasing D_e and with decreasing temperature difference between the lower and upper surface (cloud). Also, the peak BTD occurs for an upper cloud optical depth τ_1 between 1 and 2. Any *BTD* signal from the upper cloud is essentially gone for all D_e at τ_1 > 10. For larger D_e, there appears to be little information in the *BTD* for τ_1 > 2. Thus, any detection of multi-leveled clouds using the BTD will be limited by the separation of the two cloud layers and the particle size and τ of the cirrus cloud. The mean 0.3° *BTDs* for all of the VISST cloud retrievals

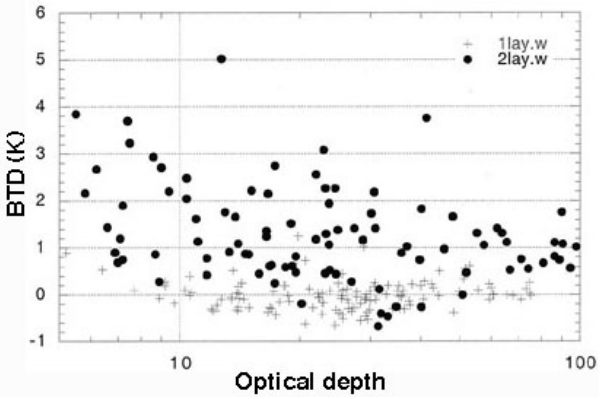

Fig. 3. Variation of mean BTD in 0.3° box from GOES-8 for 1 and 2-layered clouds identified as liquid water.

identified as being 100% liquid water are shown in Fig. 3 and categorized by the radar data as being either 1 or 2 layers. BTD for the single-layered clouds is less than 0.5 K for most of these cases, while *BTD* exceeds 0.5 K for a large majority of 2-layered cases. No single-layer cloud has a *BTD* greater than 1.5K.

The layer separation for the water clouds can be contrasted with the results in Fig. 4 for the clouds identified by VISST as being composed entirely of ice crystals. While, on average, *BTD* for the 2-layer clouds exceeds its single-layer counterpart, the values for both categories overlap considerably making it difficult to distinguish between single- and multi-layered clouds. Additionally, fewer *BTD*s greater than 2 K are seen for the ice clouds compared to those for the water clouds. This difference may be due to having a larger ice cloud optical depth for the cases identified as ice compared to those that are classified as water clouds. The VISST selects phase based on the temperature and how well the observed 3.7 and 11 µm temperatures match between model calculations for the ice and water models. The result for mixed phase and overlapped clouds is usually a selection of water phase when τ_1 is small and ice phase for larger upper-cloud optical depths. Thus, fewer large *BTD* values would occur for the ice clouds identified as 2-layer clouds. The larger values of *BTD* for the optically thick, 1-layer ice clouds in Fig. 4 compared to those in Fig. 3 may be due to the

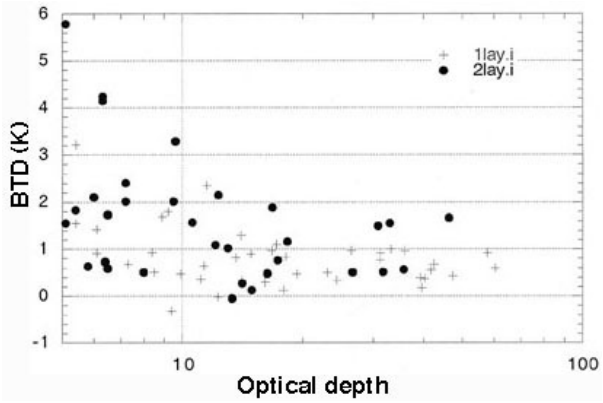

Fig. 4. Same as Fig. 3, except for ice clouds only.

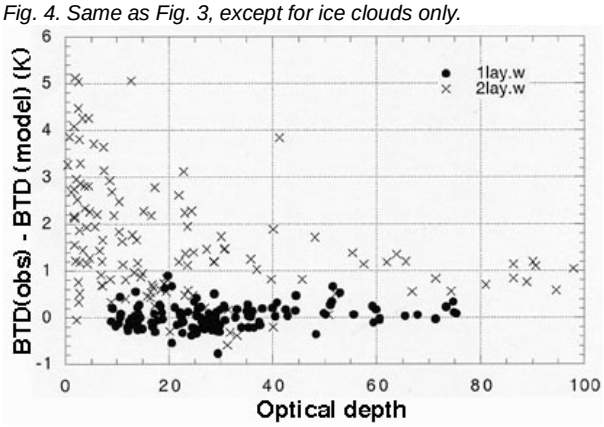

Fig. 5. Difference in BTD from GOES and from model calculations using VISST-retrieved parameters.

often great physical thickness of cirrus clouds compared to denser liquid water clouds. The great vertical variation of temperature and microphysical properties in the low-density cirrus clouds may be enough to account for *BTD* = 1 K.

If the observed cloud is single-layered, then the observed value of *BTD* should be close to that from the model calculations based on the derived values of T_c, τ, and particle size. Figure 5 shows a plot of the differences between the observed and modeled BTDs based on the retrieved properties for a single-layer cloud. The result provides even greater separation between the 1 and 2-layer clouds. An optical depth-dependent threshold could successfully detect most of the 2-layer clouds in this case. As seen in Fig. 6, the results for ice clouds are less encouraging. The large physical thickness of the cirrus clouds makes it more difficult to accurately portray cirrus as plane-parallel, single-temperature clouds in the model calculations.

Figures 7 and 8 plot the values of r_e and D_e, respectively, as functions of cloud optical depth. In general, the values of r_e for single- and multi-layered clouds overlap, except for $r_e > 15$ µm. A test using $r_e > 15$ µm would only identify only one of the single-layered clouds in Fig. 7 as a multilayered case. This test would not be as effective as a test using the results in Fig. 5, because fewer multilayered clouds would be detected.

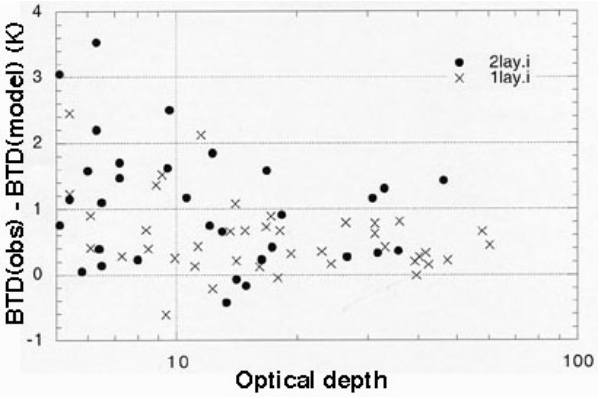

Fig. 6. Same as Fig. 5, except for ice clouds.

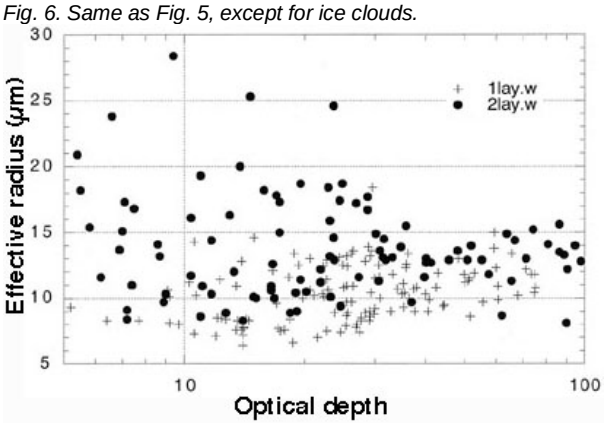

Fig. 7. Variation r_e with derived optical depth for liquid-water clouds.

On the other hand, the effective diameters derived for the multilayered clouds are much smaller than most of those for the single-layered cases. The average D_e for the multilayered clouds is approximately 80 µm compared to ~31 µm for the multilayered cases. An optical-depth-dependent threshold of 50 µm at $\tau = 0$ and 80 µm at $\tau = 100$ would detect nearly 90% of the multilayered cases while misclassifying less than 10% of the single-layered cases. Two of the cases with $D_e < 20$ µm for $\tau > 30$ may be liquid water clouds that were misclassified as ice clouds. Some of the outlying points require more detailed examination to explain their existence.

4. DISCUSSION AND CONCLUDING REMARKS

It is encouraging that many of the two-layer cloud systems appear to be identifiable in parameters that are part of the standard output from a single-layer retrieval method. Thus it should be possible to devise a simple technique for identifying those pixels that contain multilayered clouds. It is recognized that the cases studied here are somewhat idealized in that only well-separated, two layer systems were examined. Other cloud combinations will likely produce less distinct signatures. Also, the demarcation between single- and

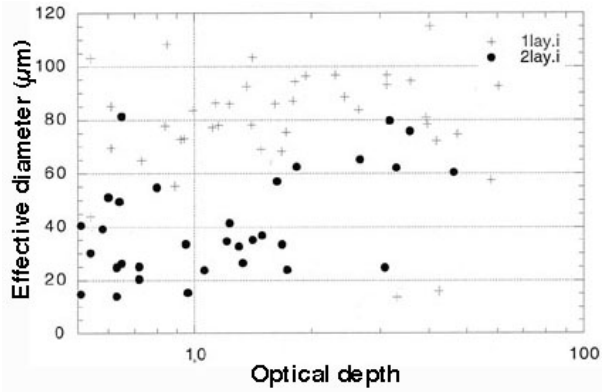

Fig. 8. Variation D_e with derived optical depth for liquid-water clouds.

two-layered clouds in the variation of r_e or D_e may change with location. For example, cloud droplets in pristine marine areas are often larger than those over land or in polluted oceanic boundary layers. Thus, the multilayer threshold for r_e may be larger over those areas than seen in Fig. 7. Such regional effects will require further exploration.

The results shown here are based on average values for relatively large areas. Ideally, a multilayer detection method should work at the pixel level, determining whether each radiance is due to one or two cloud layers. Initial thresholds will be developed from the results presented here and used to classify pixels in VISST retrievals over the ARM SGP site from GOES-8 data taken during 2000. These will be compared to similar analyses of the lidar and radar datasets over the site to determine the quality of the detection method. Data taken over other ARM sites in the tropical Pacific and over the North Slope of Alaska will also be analyzed to determine how these parameters vary with cloud layering in those very different environments. It should then be possible to develop a simple classification technique based on operational retrieval products to classify clouds as single or multilayered. The more challenging work of unscrambling the properties of the clouds in the two layers (e.g. Arduini et al. 2002) will then be applied in a more reliable fashion to generate a more complete cloud climatology from satellite remote sensing.

REFERENCES

Arduini, R. F., P. Minnis, and D. F. Young, 2002: Investigation of a visible reflectance parameterization for determining cloud properties in multi-layered clouds. *Proc. AMS 11th Conf. Cloud Physics*, Ogden, UT, June 3-7.

Baum. B. A. and J. D. Spinhirne, 2000: Remote sensing of cloud properties using MODIS airborne simulator imagery using SUCCESS, 3: cloud overlap. *J. Geophys. Res.*, **105**, 11793-11801.

Clothiaux, E. E., T. P. Ackerman, G. G. Mace, , K. P. Moran, R. T. Marchand, M. A. Miller and B. E. Martner, 2000: Objective determination of cloud heights and radar reflectivities using a combination of active remote sensors at the ARM CART sites. *J. Appl. Meteorol.*, **39**, 645-665.

Dong, X., P. Minnis, G. G. Mace, W. L. Smith, Jr., M. Poellot, and R. T. Marchand, 2002: Comparison of stratus cloud properties deduced from surface, GOES, and aircraft data during the March 2000 ARM Cloud IOP. Accepted *J. Atmos. Sci*.

Han, Q-Y., W. B. Rossow, and A. A. Lacis, 1994: Near-global survey of effective cloud droplet radii in liquid water clouds using ISCCP data. *J. Climate,* **7**, 465-497.

Inoue, T., 1985: On the temperature and effective emissivity determination of semi-transparent cirrus clouds by bi-spectral measurements in the 10 μm region. *J. Meteor. Soc. Japan*, **63**, 88-98.

Lin, B., P. Minnis, B. A. Wielicki, D. R. Doelling, R. Palikonda, D. F. Young, and T. Uttal, 1998: Estimation of water cloud properties from satellite microwave and optical measurements in oceanic environments. II: Results. *J. Geophys. Res.*, **103**, 3887-3905.

Minnis, P., D. P. Garber, D. F. Young, R. F. Arduini and Y. Takano, 1998: Parameterizations of reflectance and effective emittance for satellite remote sensing of cloud properties. *J. Atmos. Sci.*, **55**, 3313–3339.

Minnis, P. et al., 1995: Cloud Optical Property Retrieval (Subsystem 4.3). In *Clouds and the Earth's Radiant Energy System (CERES) Algorithm Theoretical Basis Document, Volume III: Cloud Analyses and Radiance Inversions (Subsystem 4)*, *NASA RP 1376 Vol. 3*, edited by CERES Science Team, pp. 135-176.

Minnis, P., W. L. Smith, Jr., and D. F. Young, 2001: Cloud macro- and microphysical properties derived from GOES over the ARM SGP domain. *Proceedings of the ARM 11th Science Team Meeting*, Atlanta, GA, March 19-23, 11 pp. (available at http://www.arm.gov/ docs/ documents/technical/conf_0103/minnis-p.pdf).

Tian, L. and J. A. Curry, 1989: Cloud overlap statistics. *J. Geophys. Res.*, **94**, 9925-9935.